Cirrus Particle Size Measurements Using A High Spectral Resolution Lidar

Ralph E. Kuehn and Edwin W. Eloranta

University of Wisconsin-Madison
1225 West Dayton St.
Madison, WI 53706

Tel: +608-262-7327 • Fax: +608-262-0166
Email: eloranta@lidar.ssec.wisc.edu

ABSTRACT

High Spectral Resolution Lidar (HSRL) measurements of cirrus cloud extinction and multiple scattering are used to determine cloud effective particle size. The multiple scattered lidar return depends on the following parameters: 1) the transmitter divergence, 2) the receiver field-of-view, 3) the cloud extinction profile, 4) the effective radius, and 5) the backscatter phase function. This technique relies on the HSRL's ability to measure the extinction cross-section and multiple scattered photons which have been backscattered from molecules. An approximate analytic model is used to calculate the multiple scatter contribution using the molecular backscatter phase function and the HSRL-measured extinction profile for different particle sizes. The HSRL molecular-backscattered multiple scattering data are then compared to the model results to find the particle size which provides the best fit.

1. INTRODUCTION

Here we demonstrate a new method of measuring cirrus cloud effective particle size from lidar multiple scattering and extinction measurements, using the University of Wisconsin High Spectral Resolution Lidar (HSRL).[1,2] The effective radius is determined by measuring the width of the diffraction peak from HSRL multiple field-of-view molecular backscatter measurements. The molecular backscattering events depend only on the diffraction peak width and the extinction profile and do not depend on the shape or magnitude of the backscatter phase function of the cirrus particles. The multiple scattering contribution is significant in clouds because as the transmitted laser pulse travels through the cloud, half of the single scattered energy from cloud particles is contained within the forward diffraction peak. This scattered energy propagates along with the transmitted beam and contributes to the lidar signal. The diffraction peak width is inversely proportional to the number weighted average cross-sectional area times the scattering cross-section,[3] which is directly related to the effective radius of the particle size distribution.

This technique utilizes the ability of the HSRL to simultaneously measure multiple scattered photons backscattered from atmospheric molecules and cloud extinction. An approximate multiple scatter model[4] is used to calculate the multiply scattered lidar return as a function of the receiver FOV and the effective radius, given the parameters of the cloud extinction profile, receiver FOV, and transmitter divergence. Then the effective radius $r_e = \langle r^3 \rangle / \langle r^2 \rangle$, is used as a variable to optimize the fit of the model output to HSRL observations. When the model results are in agreement with the observations, the value of r_e used for the model calculations is assumed to represent r_e of the cloud.

2. DETERMINING CLOUD EXTINCTION

A profile of cloud extinction is required to run the multiple scatter model. Cloud extinction can be measured with the HSRL using two different techniques. The preferred technique used in this analysis requires that cloud

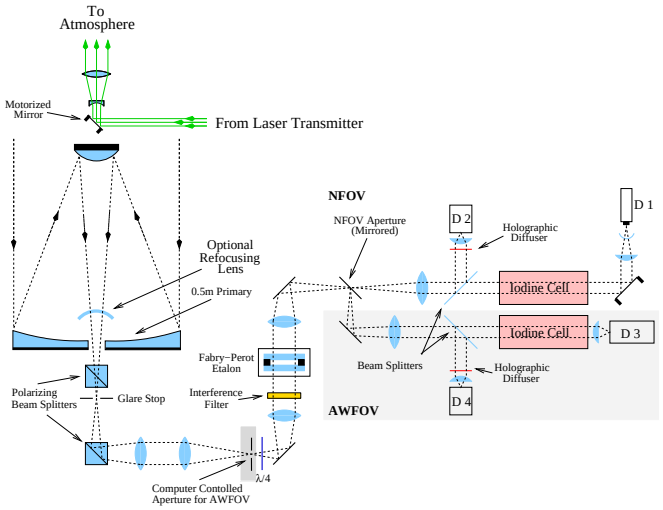

Figure 1. Diagram of the HSRL receiver. The AWFOV detectors are shown in the shaded area. The AWFOV size is set by a computer controlled aperture (also shaded) and the NFOV aperture, which is a mirror with a hole in the center.

is transparent to the lidar. An average value for the backscatter phase function can be calculated when the following equation is satisfied:

$$\int_{z_1}^{z_2} \frac{\beta'_a(z)}{\langle \frac{\mathcal{P}_a(\pi)}{4\pi} \rangle} dz = \tau_s(z_2) - \tau_s(z_1) \tag{1}$$

where $\beta'_a(z)$ is the measured backscatter cross-section, $\langle \mathcal{P}_a(\pi) \rangle / 4\pi$ is the average backscatter phase function, $\tau_s(z_2) - \tau_s(z_1)$ is the measured optical depth of the cloud, z_1 is the altitude of the cloud base, and z_2 is an altitude several kilometers above the cloud top where multiple scatter contributions to the lidar signal are small. The extinction profile, $\beta_a(z)$ is then calculated by,

$$\beta_a(z) = \frac{\beta'_a(z)}{\langle \frac{\mathcal{P}_a(\pi)}{4\pi} \rangle} \tag{2}$$

Calculating $\beta_a(z)$ in this manner minimizes errors in $\beta_a(z)$ caused multiple scattering.

3. INSTRUMENTATION: HSRL RECEIVER

This section describes features of the HSRL receiver required for multiple scattering measurements. The receiver is split into two major parts, the Narrow Field-Of-View (NFOV) channels, and the Annular Wide Field-Of-View (AWFOV) channels (see fig 1). The NFOV channels measure the single scatter lidar return, which are used to derive the backscatter cross-section, and the optical depth. The AWFOV detectors measure the multiply scattered and some single scattered energy. The signal measured by detector D3 is special because the multiple scatter contribution is significant and the Iodine absorption cell has removed photons backscattered from aerosols.

The wide FOV of the HSRL is an controlled by a mechanical aperture (iris) placed at the focal plane of the telescope which can be changed in diameter by the data acquisition system. The aperture diameter is changed after every averaging period which is on the order of three seconds. The AWFOV aperture cycles through four different diameters/FOVs (i.e. 0.3, 0.5, 1.0, 2.0, 0.3, 0.5... $m$rad). This is done to simplify data analysis and to minimize the effect of cloud variability.

4. THE AWFOV RATIO EQUATION

The signal collected by AWFOV channel contains some single scattered energy so it was necessary to subtract this single scattered energy before the result can be compared to the model output. The AWFOV ratio is defined

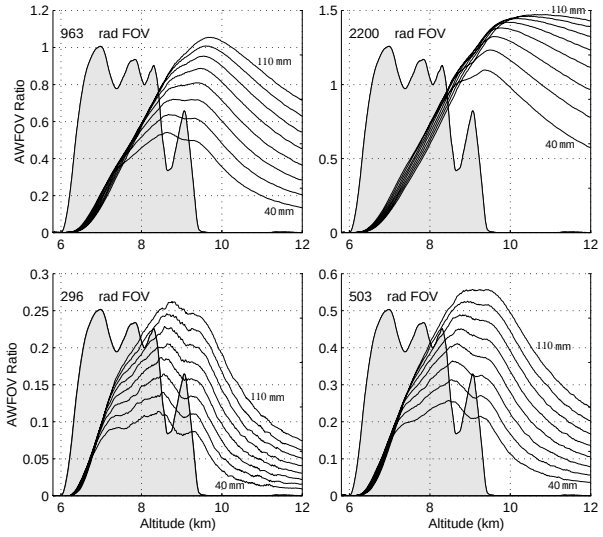

Figure 2. Multiple scatter model AWFOV ratios, $G(z)$, computed for the extinction profile observed on February 22, 2001, 02:17-02:41 UT. Results are shown for each FOV and effective radii ranging from 40-110 μm in intervals of 10 μm. The shaded area is the profile of the backscatter cross-section, $\beta'_a(z)$, shown for reference. $\beta'_a(z)$ is plotted on a linear scale, with a maximum observed value of $8.5 \cdot 10^{-6}$ $(m^{-1} \cdot sr^{-1})$.

as:

$$G(z) = \frac{N_\Psi(z) - kN_\theta(z)}{N_\theta(z)} \left(\frac{C_\theta}{C_\Psi} \right) \tag{3}$$

where,

$$k = \frac{C_\Psi}{C_\theta} \frac{e_\Psi}{e_\theta} \tag{4}$$

$N_\Psi(z)$ and $N_\theta(z)$ are the number of photons received in the AWFOV and NFOV channels, respectively, as a function of range. C is the detector efficiency and optical transmission factor for each FOV and must be determined from system calibrations in order to scale the ratios properly for comparison to the model output. Finally, e represents the fraction of energy transmitted within each FOV.

5. RESULTS

On February 22, 2001 the HSRL collected data from 01:14 UT until 04:53 UT, in Madison, Wisconsin. During this period the AWFOV aperture was operated to collect multiple scattering data. High altitude ice clouds were observed during this period.

Since the multiply scattered signal backscattered by molecules is quite small, the data must be averaged to ensure that the statistical errors (photon counting) are small. In this case 24 minutes were required to reduce statistical errors to an acceptable level. The averaging period was from 02:17:36 until 02:41:22 UT. During this period the cloud base remained relatively constant and uniform. Also, the region below the cloud layer was free from other cloud layers.

The results from the model run of February 22, 2001 are summarized by figure 2 which shows the AWFOV ratios, $G(z)$. The average value of r_e during the period 02:17-02:41 UT was determined to be 70μm. This is based on the comparison of the model and HSRL values of the AWFOV ratios shown in figure 3. For the three largest FOV the agreement with the model results appears quite good and is within statistical error limits computed for the HSRL derived ratios. The comparison with the smallest AWFOV however, shows a considerable discrepancy. This is because the AWFOV aperture steps from the largest FOV to the smallest while the system is acquiring

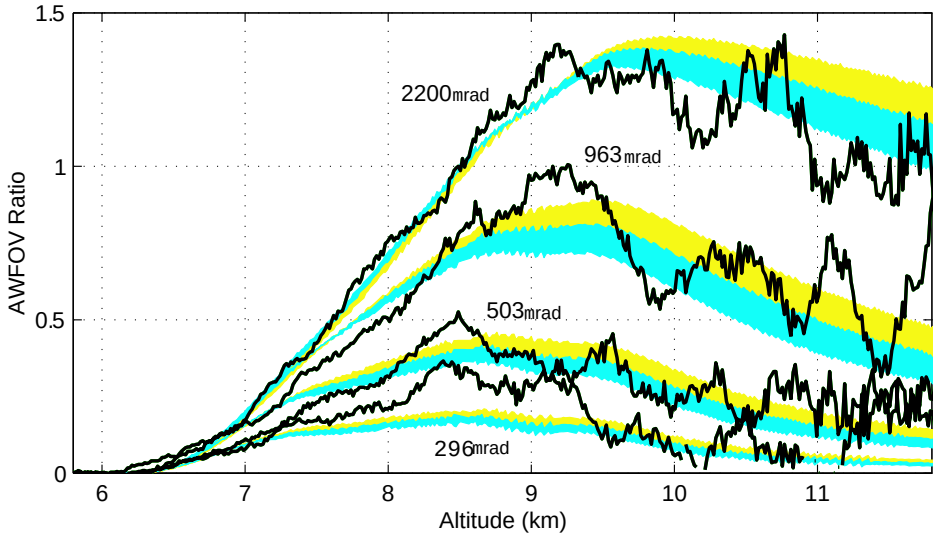

Figure 3. HSRL AWFOV ratios, $G(z)$, for the period 02:17-02:41 UT, compared to the multiple scattering model results. The shaded curves represent the model results where r_e ranges from 60 to 80 μm, in 10 μm intervals. The HSRL derived ratios (solid lines) are plotted at a vertical resolution of 15 m, and were smoothed with a 21 bin (315 m) moving average filter.

data, so the effective FOV for that averaging period is larger than 296 μrad used to produce the model results. This issue can be resolved by modifying our data collection procedure.

ACKNOWLEDGMENTS

We would like to thank Robert Holz for his help collecting the HSRL data. This work was supported by DOE grant #DE-FG02-00ER62968

REFERENCES

1. P. Piironen and E. W. Eloranta, "Demonstration of a high-spectral-resolution lidar based onan iodine absorption filter," *Opt. Lett.* **19**, pp. 234–236, 1994.
2. P. Piironen, *A High Spectral Resolution Lidar Based on an Iodine Absorption Filter*. PhD thesis, University of Joensuu, Finland, 1994.
3. H. C. van de Hulst, *Light Scattering by Small Particles*, John Wiley and Sons, New York, N.Y., 1957. Reprinted 1981 by Dover Publications, New York, N.Y.
4. E. W. Eloranta, "Practical model for the calculation of multiply scattered lidar returns," *Appl. Opt.* **37**, pp. 2464–2472, 1998.